Water Splitting Using Electrochemical Approach

Akira Yamaguchi, Toshihiro Takashima, Kazuhito Hashimoto and Ryuhei Nakamura

Abstract For electrochemical water splitting, a number of bioinspired and biomimetic Mn-based materials have been developed; however, the catalytic performances markedly differ between natural and synthetic Mn catalysts. Based on the recent in situ detection of surface intermediates for the oxygen evolution reaction (OER) by MnO_2, this chapter introduces the design rationale for the efficient OER catalysts, and discusses the evolutional origin of natural Mn_4-clusters to provide a better understanding of the differences in activity between natural and man-made OER catalysts.

1 Introduction

Water is by far the most abundant source of electrons in nature. In biological systems, plants, algae, and cyanobacteria utilize water as the primary electron source to maintain cellular function and growth, thereby contributing to homeostasis and sustainable ecosystems. For humans to mimic such sustainable natural systems, the development of artificial water splitting systems that efficiently utilize water as an electron source is needed for generating renewable fuels [1–4]. In particular, relatively clean water at neutral pH is the most desirable resource, as it is abundant and safe for handling. However, artificially extracting electrons from water requires excess energy owing to the inherent difficulty of catalyzing the

A. Yamaguchi · R. Nakamura (✉)
Biofunctional Catalyst Research Team, RIKEN Center for Sustainable Resource Science, 2-1 Hirosawa, Wako, Saitama 351-0198, Japan
e-mail: ryuhei.nakamura@riken.jp

T. Takashima
Clean Energy Research Center, University of Yamanashi, Kofu, Yamanashi 400-8511, Japan

K. Hashimoto
Department of Applied Chemistry, The University of Tokyo, 7-3-1 Hongo, Bunkyo-ku, Tokyo 113-8656, Japan

M. Sugiyama et al. (eds.), *Solar to Chemical Energy Conversion*, Lecture Notes in Energy 32, DOI 10.1007/978-3-319-25400-5_11

overall four-electron/four-proton reaction, known as the oxygen evolution reaction (OER) ($2H_2O \rightarrow 4H^+ + 4e^- + O_2$). In contrast, the tetrameric Mn cluster of photosystem II (PSII) in photosynthetic organisms catalyzes the OER with remarkably high activity and selectivity, as demonstrated by the overpotential values of 160–300 mV [5–7] and maximum turnover frequencies of $\sim 10^3\ s^{-1}$ [8].

Inspired by natural water-splitting catalysts, OER catalysts composed of Mn, which is an inexpensive and abundant element, have attracted considerable research interest. A number of bioinspired and biomimetic Mn-based materials have been developed as water-splitting catalysts; however, the catalytic performances markedly differ between natural and synthetic Mn catalysts, particularly under neutral pH conditions. Despite intensive studies aiming at understanding the catalytic process of natural and artificial catalysts, the reasons underlying the differences in ability are unclear. Furthermore, the fundamental question as to why Mn is the only element found in nature that is capable of efficient water splitting remains unanswered. This question is particularly relevant to the evolution of PSII, as oxygen reduction reactions in respiration ($O_2 + 4H^+ + 4e^- \rightarrow 2H_2O$), which is the reverse reaction of the OER and operates at essentially the same potential region with OER (1.23 V vs. RHE), exploit several metal elements, such as Fe and Cu, but not Mn, as catalytic centers.

To help resolve the above questions, this chapter describes recent development in OER catalysts designed based on electrochemical systems, particularly focusing on MnO_2-based catalysts. First, a brief overview of electrochemical OER catalysts, including a comparison of Mn-, noble metal-, and Co-based catalysts, is presented in Sects. 2 and 3. In Sect. 4, the results of spectroscopic examination of MnO_2-based OER catalysts are presented, and the importance of Mn^{3+} in the overall water-splitting reaction is discussed. Based on these findings, the origin of the differences in activity between natural and man-made MnO_2 OER catalysts is discussed in Sect. 5. In Sect. 6, a strategy for controlling proton transfer and improving the catalytic activity of MnO_2 for OER under neutral pH conditions is proposed. In the final section, perspectives related to the evolutional origin of natural Mn_4-clusters are described.

2 Electrochemical Water Oxidation Catalysts with 3d-Block Elements

To achieve high catalytic activity for the electrochemical OER, a number of noble metals, such as Ir and Ru, have been adopted as catalysts. For example, in 1971, Trasatti et al. [9] reported that a RuO_2 film electrode prepared on titanium exhibited high OER activity, with an overpotential at 10 mA cm^{-2} of 200 mV in 1 M $HClO_4$. This finding inspired the development of a number of colloidal and heterogeneous RuO_2-based OER catalysts [10, 11]. However, despite their high catalytic activity, RuO_2-based catalysts exhibit anodic corrosion at high anodic potential, thereby limiting their practical application.

IrO_x are potentially suitable candidates for OER catalysts as they exhibit both high catalytic activity and stability [10, 12, 13]. Yagi et al. [14] reported that a monolayer of citrate-stabilized IrO_2 nanoparticles (50–100 nm) deposited on an ITO electrode had catalytic water oxidation activity with an onset potential of 1.2 V vs. SHE at pH 5.3. Furthermore, by decreasing the particle size (1.6 ± 0.6 nm), the catalytic activity of IrO_2 drastically increased, with an overpotential of 150–250 mV at 0.5 mA cm^{-2} over a pH range of 1.5–13, and showed a current efficiency of 100 % at an overpotential of 250 mV at 0.5 mA cm^{-2} [15, 16]. Although these catalysts displayed high catalytic activity and durability over a wide range of pH, the high cost and scarcity of noble metals severely limit their widespread use as water-splitting catalysts. Thus, a distinct need exists for more abundant materials that can serve as efficient catalysts in such systems.

For the utilization of abundant elements, particularly 3d-block transition metal elements, as OER catalysts, it is necessary to understand the mechanisms underlying OER activity from a theoretical perspective [17–19]. One possible determinant of OER activity is metal ion (M)–OH bond strength. In the early 1950s, Rüetschi et al. [17] theoretically investigated the OER under alkaline conditions with several types of noble metal and 3d-block transition metal electrodes, including electrodes composed of Ag, Au, Cd, Co, Cu, Fe, Ni, Pb, Pd, and Pt, and found that the overpotential for OER linearly decreases with increasing M–OH bond energy.

Another potential determinant is the occupancy of the e_g orbital in active metal sites. Iwakura et al. [18] reported that OER activity of transition metal oxides with spinel structures ($Co_xFe_{3-x}O_4$, $Mn_xFe_{3-x}O_4$, and $Ni_xFe_{3-x}O_4$) increases with increasing number of unpaired d-electrons when the rate-determining step is the generation of OH radical via oxidation of OH^- ($HO^- \rightarrow HO^{\bullet} + e^-$), but decreases with increasing number of unpaired d-electron if the rate-determining step is the reaction between OH radical and OH^-. Bockris et al. [19] investigated the relationship between OER activity and multiple factors, such as the effective magnetic moment, formation enthalpy of the corresponding hydroxides, M–OH bond strength, and d-electron numbers, of 18 perovskite-type oxides. The authors concluded that OER activity is related to the occupancy of the antibonding orbitals of M–OH and predicted a volcano plot for OER efficiency as a function of M–OH bond strength. Motivated by these theoretical studies and the success of d-band modeling to predict catalytic activity, in 2011, Shao-Horn et al. [20] investigated the OER activity of $Ba_{0.5}Sr_{0.5}Co_{0.8}Fe_{0.2}O_{3-\delta}$, which has a perovskite structure, and found this compound catalyzes the water oxidation reaction under alkaline conditions with an overpotential of 250 mV at current density of 50 μA cm^{-2}. In addition, these researchers investigated the OER activities of more than 10 metal oxides and found that the activity showed a volcano-shaped dependence on the electron occupancy of an e_g orbital of surface transition metal cations [20]. The highest predicted catalytic activity based on volcano plots was for the $Ba_{0.5}Sr_{0.5}Co_{0.8}Fe_{0.2}O_{3-\delta}$-based catalyst, which possesses one electron in its 3d e_g orbital (Fig. 1). Taken together, these studies demonstrate that the d-band model is effective for the rational design of OER catalysts comprised of 3d-block transition metal elements under alkaline conditions [17–20].

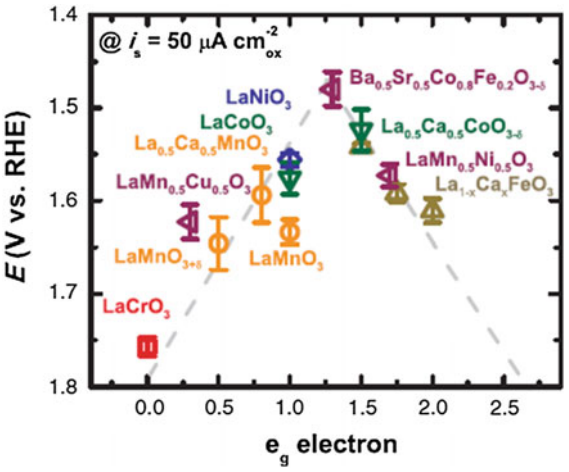

Fig. 1 The volcanic relation between the OER activity, defined by the overpotentials at 50 μA cm^{-2} $_{ox}$ of the OER current, and the occupancy of the e_g-symmetry electron of the transition metal (B in ABO_3) under alkaline condition [20]

It is important to note, however, that predicted catalytic efficiencies based on d-band models are not always applicable for the neutral pH conditions. For example, Raabe et al. [21] examined the surface conditions of $Pr_{1-x}Ca_xMnO_3$ (PCMO) during the OER at pH 7 by in situ transmission electron microscopy (TEM) and revealed that an amorphous PCMO layer formed with a concomitant decrease of OER activity. Furthermore, in situ electron energy-loss spectroscopy (EELS) analysis revealed that the oxidation state of the Mn site was reduced to 2.0 from the initial value of 3.2 during the reaction. This tendency for the deterioration of OER activity at neutral pH cannot be directly explained by the d-band model and is most likely because the overall rate-determining step is the storing process of oxidative power, not the downstream reactions, such as H_2O adsorption and O-O bond formation, as discussed in Sect. 4.

Among 3d-block transition metal elements, the OER catalytic efficiency of soluble aquo and hydroxo complexes of CoO_x has been widely investigated under both heterogeneous and homogeneous conditions at neutral pH since the early 1980s [22–24]. In 2008, Nocera et al. [23] reported the in situ formation of a catalytic film composed of cobalt phosphates, hydroxide, and oxides from a neutral solution of Co(II) and phosphate ions upon application of a positive potential to an ITO electrode. This film catalyst exhibited OER activity with an overpotential of 410 mV at 1 mA cm^{-2} at pH 7. In 2009, a preparation of cubic Co_3O_4 nanoparticles (5.9 ± 1.0 nm) showed an electrochemical OER current density of 10 mA cm^{-2}, with an overpotential of 330 mV, under alkaline conditions [24]. Although these Co-based materials display high catalytic activity even at neutral pH, as is the case for IrO_2, which are active over a wide pH range, Mn-based OER catalysts exhibit low activity under neutral pH conditions, as described in the following section.

3 Manganese-Based Catalysts Inspired by the Natural Oxygen-Evolving Center

Inspired by the natural O_2 evolution center, large numbers of Mn-based water oxidation catalysts, including metal complexes and bulk oxides such as MnO_2, Mn_2O_3, and MnOOH, have been investigated [25–43]. Mn-based catalysts demonstrate high OER activity under alkaline conditions. For example, a complex metal oxide $MnFe_2O_4$ catalyzes electrochemical OER in 1 M KOH at an overpotential of 400 mV at 100 mA cm^{-2} [42], and similarly, nanostructured MnOOH electrodeposited on a gold electrode at pH 14 with an overpotential of 390 mV at 50 mA cm^{-2} [27]. In addition, efficient OER catalytic activity was demonstrated for Mn_2O_3 with an overpotential of 290 mV at 1 mA cm^{-2} at pH 14 [28].

Despite the high catalytic OER activity of Mn-based catalysts under alkaline conditions, their activity dramatically decreases at neutral pH. This response was clearly demonstrated by Tamura et al. [29], who examined the OER activity of MnO_2 electrocatalysts that were synthesized on Ti or Pt electrodes by the thermal decomposition of $Mn(NO_3)_2$ under highly acidic (1 N H_2SO_4), highly alkaline (1 N KOH), and neutral (1 N K_2SO_4) conditions. Although the electrodes exhibited high catalytic activity under alkaline and acidic conditions, with an overpotential of 300 mV at 1 mA cm^{-2}, the activity was markedly lower under neutral conditions, with overpotential of 610 mV. This tendency has also been observed with other Mn-based materials, including MnOOH and Mn_2O_3 [26, 28]. Therefore, the catalytic OER activity of Mn-based catalysts varies drastically between alkaline and neutral pH.

4 Electrospectroscopic Examination of Manganese Oxide Water Oxidation Catalyst

To determine why synthetic Mn catalysts show a sharp decline in catalytic activity under neutral conditions, we recently performed a spectroelectrochemical characterization of intermediate species of the OER for an MnO_2 electrode [44–46]. During the OER at neutral pH, a new absorption band with a maximum around 510 nm was observed at the potential slightly negative than the onset for OER. Utilizing pyrophosphate as a probe molecule, the new absorption peak was assigned to the d-d transition of Mn^{3+} that was generated via the injection of electrons from water to MnO_2. We also examined the pH dependence of the onset potential of the water oxidation current on the MnO_2 electrode and found that under neutral conditions (pH 4–8), the onset potential for OER remained constant at approximately 1.5 V vs. SHE, whereas it sharply shifted in the negative direction and showed

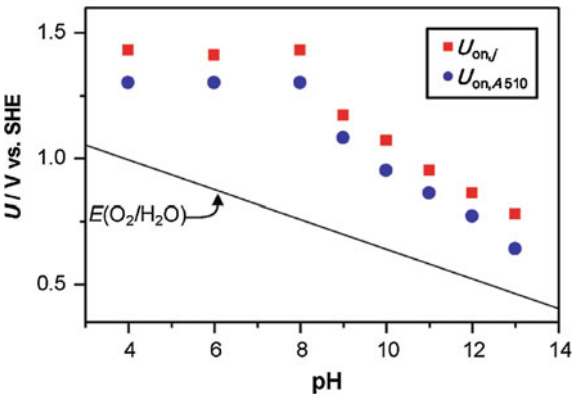

Fig. 2 pH dependences of the onset potential for oxidation current ($U_{on,j}$, *squares*) and optical absorption at 510 nm ($U_{on,A510}$, *circles*). The *solid line* represents the standard potential for OER [44]

linear pH-dependent behavior under alkaline conditions (Fig. 2). Notably, the OER current was accompanied by the appearance of the d-d transition absorption of Mn^{3+}, indicating that Mn^{3+} acts as an intermediate for the OER. However, Mn^{3+} is unstable at neutral pH due to charge disproportionation ($2Mn^{3+} \rightarrow Mn^{2+} + Mn^{4+}$), but exists stably under alkaline conditions. Based on these experimental observations and the pH-dependent redox behavior of Mn^{3+}, we proposed a new model to explain the low activity of MnO_2 OER catalysts under neutral conditions (Fig. 3). In this model, electrons are injected from water to MnO_2 prior to the evolution of O_2, resulting in the formation of Mn^{3+} at the MnO_2 electrode surface. Because Mn^{3+} is unstable due to the disproportionation reaction, Mn^{2+} must be electrochemically oxidized to Mn^{3+} to sustain the catalytic turnover. The regeneration of Mn^{3+} from

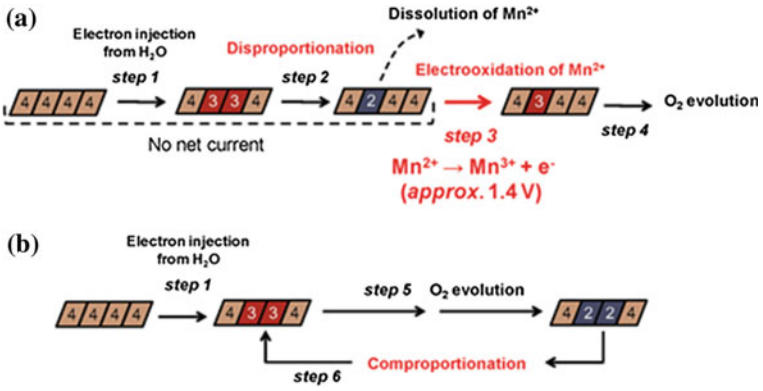

Fig. 3 Oxidation states of Mn ions involved in OER on a δ-MnO_2 electrode at **a** pH 4−8 and **b** pH ≥ 9 [44]

Mn^{2+} serves as the rate-determining step of the OER under neutral conditions. This model is supported by the experimental observation that the onset potential for OER under neutral conditions remains constant at approximately 1.5 V, as the oxidation potential of Mn^{2+} to Mn^{3+} ($Mn^{2+} \rightarrow Mn^{3+} + e^{-}$) is approximately 1.4 V regardless of the solution pH (Fig. 3). Thus, the origin of the large overpotential for the OER with MnO_2 catalysts is attributable to the inherent instability of Mn^{3+} under neutral conditions. Then the new question arises: does Mn^{3+} stably exist in the tetrameric Mn cluster of PSII during the reaction cycle, known as Kok cycle?

5 Natural Versus Man-Made MnO_2

A key process in natural photosynthesis is the four-electron/four-proton water oxidation reaction that produces O_2. This reaction occurs in the oxygen-evolving complex (OEC) of PSII. Among 3d-block transition metal elements, only Mn is utilized as a photosynthetic center in OEC [47, 48]. Similarly, in almost all photosynthetic organisms, the μ-oxo-bridged tetrameric Mn cluster $CaMn_4O_5$, functions as an OEC [47]. This Mn_4-cluster catalyzes the oxidation of water to molecular oxygen with a low overpotential (160–300 mV) [5–7] and high turnover frequency (maximum 10^3 s^{-1}) under mild conditions [8]. The catalytic cycle of the Mn_4-cluster has been extensively investigated both spectroscopically and computationally [49–56]. In the Kok cycle, the OEC is sequentially oxidized by four photogenerated oxidizing equivalents. Although the oxidation states of the intermediates, which are denoted as S_n states (n = 0 − 4), are still debated, they are commonly assigned from S_0, $3Mn^{III}$ Mn^{IV}, to S_4, which is a putative $3Mn^{IV}$, Mn^{V}, or $4Mn^{IV}$-ligand radical that promotes O−O bond formation and O_2 release. In the Kok cycle, Mn^{III} exists stably in spite of the fact that Mn^{3+} is vulnerable to charge disproportionation in man-made Mn catalysts (Fig. 3). Therefore, the regulation between charge comproportionation ($Mn^{2+} + Mn^{4+} \rightarrow 2Mn^{3+}$) and charge disproportionation ($2Mn^{3+} \rightarrow Mn^{2+} + Mn^{4+}$) is of key importance for enhancing the OER activity of MnO_2-based materials at neutral pH. Recently, we enhanced OER activity by the formation of an N-Mn bond via coordination of the amine groups of poly(allylamine hydrochloride) to surface Mn sites of MnO_2 electrodes [45]. Using this approach, charge disproportionation is suppressed by the introduction of asymmetry into the Mn-centered crystal field, thereby eliminating the orbital degeneracy of Mn^{3+} ($t_{2g}^3 e_g^1$). Nevertheless, the molecular mechanisms behind the stabilization of Mn^{3+} relative to charge disproportionation in OEC is largely unknown. The knowledge developed in charge ordering of perovskite materials may provide new insight in this subject [57, 58].

6 Strategy for Efficient Manganese Oxide-Based Water Oxidation Under Neutral Conditions

In Sect. 4, we described a reaction model for the OER mechanism of MnO_2 catalyst, and proposed a strategy to increase the catalytic activity based on this model in Sect. 5. In the reaction model, the onset potential for OER of MnO_2 catalyst under neural conditions is determined by the regeneration of Mn^{3+} from the Mn^{2+} generated in the disproportionation reaction [44–46]. On examination of the pH dependence of the onset potential, it is clear that the reaction mechanism changed at a pH of approximately 10 (Fig. 2). It is important to note that the pK_a of the coordinated water ligand of Mn^{2+} is 10.6 [59], indicating that the protonation state of the ligand changes at around pH 10; i.e., the ligand is protonated at neutral pH and deprotonated at alkaline pH. However, because the pK_a of the coordinated water ligand of Mn^{3+} is reported to be 0.7 [59], the water ligand exists in the deprotonated state over a wide pH range. As the onset potential for OER was shown experimentally to be pH-independent under neutral conditions (Fig. 2), the regeneration of Mn^{3+} from Mn^{2+} proceeds via Mn^{3+}-OH_2, because proton transfer is not involved in the rate-determining step. Thus, the regeneration of Mn^{3+} is not a proton-coupled process, rather, it involves the sequential transfer of electrons and protons.

In contrast to the sequential electron/proton transfer step in man-made MnO_2 OER catalysts, the amino acid residues coordinating to the Mn_4-cluster in PSII construct a complex hydrogen-bonding network and regulate the transfer of protons generated in the water oxidation reaction [47, 60, 61]. Moreover, proton transfer is coupled to electron transfer in each oxidizing step of the Kok cycle [56]. Therefore, proton transfer is involved in the catalytic cycle of the natural enzyme, but it is absent in the rate-determining step of the OER by man-made MnO_2 catalysts. Based on this difference, the control of proton transfer appears to be one of the reasons for the higher catalytic activity of Mn_4-clusters. If this is the case, the OER catalytic activity of man-made catalysts can be enhanced by induction of concerted proton-coupled electron transfer (CPET) [62], as occurs in the OEC of natural systems.

As a strategy to induce CPET in artificial MnO_2 catalysts, we focused on the libido rule of acid-base catalysis [63–65], which was proposed by Jencks in 1972 [64] and states that *general acid-base catalysis of reactions coupled to proton transfer (PT) in aqueous solution can occur only at sites that undergo a large change in pK_a in the course of the reaction and when this change in pK_a converts an unfavorable to a favorable PT with respect to the catalyst; i.e., the pK_a of the catalyst is intermediate between the initial and final pK_a values of the substrate site*. Based on this rule governing acid-base catalytic reactions, we anticipated that CPET would be induced by the addition of base reagents with a pK_a between those of Mn^{2+}–OH_2 (10.6) and Mn^{3+}–OH_2 (0.7) (Fig. 4).

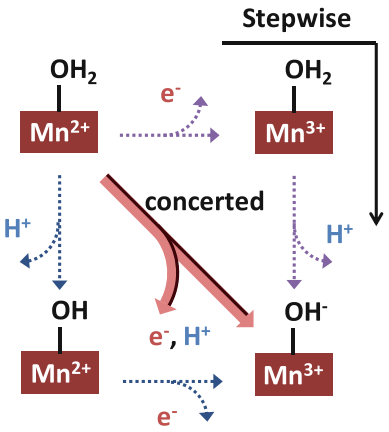

Fig. 4 Electrooxidation of Mn^{2+} to Mn^{3+} on the surface of MnO_2 electrodes

As possible CPET inducers, we selected pyridine because of its relatively high durability for electrochemical oxidation. Introducing pyridine into the electrolyte solution enhanced the electrochemical OER activity of the MnO_2 electrode, as demonstrated by the 200 mV decrease in an overpotential and markedly enhanced current density. Importantly, the onset potential for the OER showed clear pH dependence under neutral conditions, but were nearly constant in the absence of pyridine. This behavior indicates that introduction of the base reagent induced proton transfer in the rate-determining step, as was predicted from the libido rule. The induction of simultaneous electron and proton transfer reactions is also supported by the experimental observation that the kinetic isotope effect, which is determined by the ratio of current density under H_2O to that under D_2O and is defined at 1.29 V vs. SHE and the predicted degree of proton transfer that occurs in the rate-determining step, were both increased by the addition of pyridine to the MnO_2-based catalytic system.

To achieve even higher OER activity, we selected several candidate pyridine derivatives with pK_a's higher than that of pyridine with the expectation that proton transfer would be accelerated due to the stronger proton-extracting ability of the derivatives. Upon addition of the methyl group-substituted pyridines 3-methylpyridine (β-picolline), 4-methylpyridine (γ-picolline), 2,6-dimethylpyridine (2,6-lutidine), and 2,4,6-trimethylpyridine (γ-collidine), into the electrolyte solution of the MnO_2 catalyst, the OER activity increased with increasing pK_a value (Fig. 5) and was found to approximately half of that observed under alkaline conditions in the presence of γ-collidine. In addition, the KIE also increased with increasing pK_a value. Taken together, these results indicate that bases with higher proton-extracting ability promote greater proton transfer in the rate-determining step and thereby increase the OER activity of the catalyst. Yet it should be noted that the base has the possibility to affect several elementary steps other than the oxidation of Mn from 2+ to 3+ in a course of electrocatalytic water oxidation.

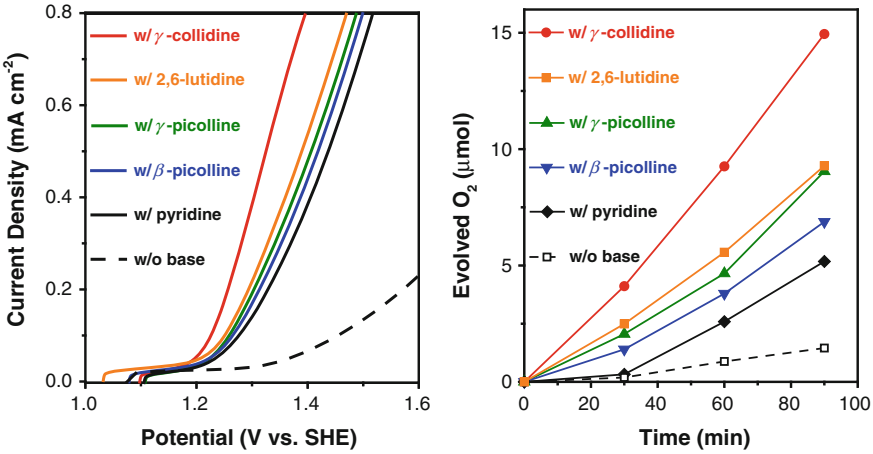

Fig. 5 *Left* Potential dependence of current density for MnO_2 electrodes in the presence of pyridine derivatives and *Right* time course of O_2 production observed for MnO_2 electrodes at an applied potential of +1.39 V versus SHE at pH = 7.5 in the presence of pyridine derivatives

7 Elemental-Based Strategy for Biological Water Splitting

In the previous sections, we described several reasons for the differences in OER activity between natural and man-made Mn-based catalysts, and introduced a strategy for enhancing the activity of the latter. In this section, we will attempt to answer why Mn was adopted for OEC in natural systems. The possible evolutionary origin of natural Mn_4-clusters has been discussed in the literature [66–68]. Russell et al. [66] suggested that the Mn_4-cluster originated from the colloidal cluster of $CaMn_4O_9{\cdot}3H_2O$ and was generated by the super-ultraviolet irradiation-induced reaction between Mn^{2+} and Ca^{2+} [66]. Sauer and Yachandra [67] compared the bond lengths of Mn–Mn in the Mn_4-cluster (2.7–2.8 and 3.3 Å) with those of several Mn-based minerals and speculated that hollandite (mainly composed of α-MnO_2) was possibly the evolutionary origin of the Mn_4-cluster due to the structural similarity between hollandite and the OEC.

As mentioned in the Introduction, the OEC does not use 3d-block elements other than Mn, unlike other enzymatic reaction centers, such as those used for O_2 reduction, even though these elements, particularly Fe, are much more abundant in nature [69]. Armstrong [68] considered that Mn was selected of natural catalytic systems because of its various oxidation states [68] and hypothesized together with Dismukes et al. [70] that the precursor for natural OEC was the Mn(II)-bicarbonate cluster in the Archean sea.

Photosynthesis is thought to have evolved 2.7 billion years ago with the emergence of cyanobacteria [71]. As a result of this activity, the O_2 concentration in ancient earth atmosphere dramatically increased 2.4 billion years ago, promoting

the evolution of multicellular organisms. In contrast, the CO_2 concentration of the earth's atmosphere gradually decreased and was not strongly correlated to the O_2 concentration. In high CO_2 environments, Mn ions predominantly exist as $MnCO_3$, but form MnO_x through reaction with O_2. Geological examination of the Kalahari Desert revealed that a critical change in mineral composition from carbonate to oxides occurred 2.3 billion years ago, [72]. The geologic stratum of the Kalahari Desert in southern Africa retains the metamorphosed record for the past $\sim$1.6–4 billion years ago, and the desert's manganese field reflects a major transition of the oxidation state of the Earth' surface. Specifically, a stratum of FeO_x was deposited over 2.7 billion years ago underneath a $MnCO_3$ layer. These findings indicate that the concentration of dissolved Mn^{2+} in shallow water could be much larger than that of Fe^{2+}, and that this difference in element availability may have led to the evolutionary selection of Mn over Fe in photosynthetic OEC systems. This constraint in element availability may have been intensified by the positive feedback manner of the photosynthetic process, as CO_2 is consumed and O_2 is produced, which would promote precipitation of Fe ions as Fe oxides.

Despite of this availability difference between dissolved Mn and Fe ions, it is possible that early photosynthetic centers adopted Fe. To examine the outcome of this selection, the bioenergetics of such systems were considered. The OER is one of the strongest oxidative reactions (E° = 1.23 V) in biological systems. Due to this property, other reactions, such as the oxidation of amino acids especially histidine, may also occur if the OER proceeds. Therefore, for PSII to have evolved, the energy gained from photosynthesis must be larger than the energy required to restore or replace the decomposed proteins. In other words, the reaction selectivity towards OER over amino acid oxidation should be sufficiently high to maintain the catalytic cycle for PSII evolution. One strategy to avoid the self-decomposition of amino acids is ligand adoption. The Mn_4-cluster is coordinated by 6 carboxylate ligands [47]. Such the high number of carboxylate ligands is unique for PSII, as other enzymatic active centers are typically surrounded by thiol or histidine groups, which are less tolerant toward oxidative decomposition than carboxylate ligands. In addition to the adaptation of carboxylate ligands, it is speculated that the autocatalytic electron transfer under protein coordination environments is an important consideration for the selective oxidation of water by OEC. Mn can induce chemical autocatalysis in the potential range of the OER of water [73, 74] and this property could be advantageous to induce multi-electron transfer for realizing highly selective OER [75]. OER is at the heart of the natural photosynthetic process, and also the efficiency-limiting reaction of artificial photosynthetic process designed to produce hydrogen through proton reduction or convert carbon dioxide to liquid fuel. Therefore, seeking the elemental-based strategy in biological water splitting will bring a new design rationale for functional analogues of the OEC for efficient and robust water splitting at neutral pH.

References

1. Fujishima A, Honda K (1972) Electrochemical photolysis of water at a semiconductor electrode. Nature 238:37–38
2. Nozik AJ (1978) PHOTOELECTROCHEMISTRY: APPLICATIONS TO SOLAR ENERGY CONVERSION. Annu Rev Phys Chem 29:189–222
3. Bard AJ, Fox MA (1995) Artificial photosynthesis: solar splitting of water to hydrogen and oxygen. Acc Chem Res 28:141–145
4. Lewis NS, Nocera DG (2006) Powering the planet: chemical challenges in solar energy utilization. Proc Natl Acad Sci USA 103:15729–15735
5. Vass I, Styring S (1991) pH-dependent charge equilibria between Tyrosine-D and the S states in photosystem ii. Estimation of Relative Midpoint Redox Potentials. Biochemistry 30:830–839
6. Geijer P, Morvaridi F, Styring S (2001) The S_3 state of the oxygen-evolving complex in photosystem ii is converted to the $S_2Y_Z^{\bullet}$ state at alkaline pH. Biochemistry 40:10881–10891
7. Metz JG, Nixon PJ, Rogner M, Brudvig GW, Diner BA (1989) Directed alteration of the D1 polypeptide of photosystem II: evidence that Tyrosine-161 is the redox component, Z, connecting the oxygen-evolving complex to the primary electron donor, P680. Biochemistry 28:6960–6969
8. Ananyev G, Dismukes GC (2005) How fast can photosystem ii split water? Kinetic performance at high and low frequencies. Photosynth Res 84:355–365
9. Trasatti S, Buzzanca G (1971) Ruthenium dioxide: a new interesting electrode material. Solid state structure and electrochemical behaviour. J Electroanal Chem 29:A1–A5
10. Harriman A, Richoux M, Christensen PA, Moseri S, Neta P (1987) Redox reactions with colloidal metal oxides. Comparison of radiation-generated and chemically generated $RuO_2 \cdot 2H_2O$. J Chem Soc Faraday Trans 1(83):3001–3014
11. Kiwi J, Grätzel M (1979) Colloidal redox catalysts for evolution of oxygen and for light-induced evolution of hydrogen from water. Angew Chem Int Ed 18:624–626
12. Harriman A, Pickering IJ, Thomas JM, Christensen PA (1988) Metal oxides as heterogeneous catalysts for oxygen evolution under photochemical conditions. J Chem Soc Faraday Trans 1 (84):2795–2806
13. Mills A, Russell T (1991) Comparative study of new and established heterogeneous oxygen catalysts. J Chem Soc Faraday Trans 87:1245–1250
14. Yagi M, Tomita E, Sakita S, Kuwabara T, Nagai K (2005) Self-assembly of active IrO_2 colloid catalyst on an ITO electrode for efficient electrochemical water oxidation. J Phys Chem B 109:21489–21491
15. Nakagawa T, Bjorge NS, Murray RW (2009) Electrogenerated IrO_x nanoparticles as dissolved redox catalysts for water oxidation. J Am Chem Soc 131:15578–15579
16. Nakagawa T, Beasley CA, Murray RW (2009) Efficient Electro-oxidation of water near its reversible potential by a mesoporous IrO_x nanoparticle film. J Phys Chem C 113:12958–12961
17. Rüetschi P, Delahay P (1955) Influence of electrode material on oxygen overvoltage: a theoretical analysis. J. Chem. Phys. 23:556–560
18. Iwakura C, Nashioka M, Tamura H (1982) Nihon Kagaku Kaishi 8:1294–1298
19. Bockris JO, Otagawa T (1984) The electrocatalysis of oxygen evolution on perovskites. J Electrochem Soc 131:290–301
20. Suntivich J, May KJ, Gasteiger HA, Goodenough JB, Shao-Horn Y (2011) A perovskite oxide optimized for oxygen evolution catalysis from molecular orbital principles. Science 334:1383–1385
21. Raabe S, Mierwaldt D, Ciston J, Uijttewaal M, Stein H, Hoffmann J, Zhu Y, Blöchl P, Jooss C (2012) In situ electrochemical electron microscopy study of oxygen evolution activity of doped manganite perovskites. Adv Funct Mater 22:3378–3388
22. Brunschwig BS, Chou MH, Creutz C, Ghosh P, Sutin N (1983) Mechanisms of water oxidation to oxygen: cobalt(iv) as an intermediate in the aquocobalt(ii)-catalyzed reaction. J Am Chem Soc 105:4832–4833

23. Kanan MW, Nocera DG (2008) In Situ Formation of an Oxygen-Evolving Catalyst in Neutral Water Containing Phosphate and Co^{2+}. Science 321:1072–1075
24. Esswein AJ, McMurdo MJ, Ross PN, Bell AT, Tilley TD (2009) Size-dependent activity of Co_3O_4 nanoparticle anodes for alkaline water electrolysis. J Phys Chem C 113:15068–15072
25. Gorlin Y, Jaramillo TF (2010) A bifunctional nonprecious metal catalyst for oxygen reduction and water oxidation. J Am Chem Soc 132:13612–13614
26. Mohammad AM, Awad MI, El-Deab MS, Okajima T, Ohsaka T (2008) Electrocatalysis by nanoparticles: optimization of the loading level and operating pH for the oxygen evolution at crystallographically oriented manganese oxide nanorods modified electrodes. Electrochim Acta 53:4351–4358
27. El-Deab MS, Awad MI, Mohammad AM, Ohsaka T (2007) Enhanced water electrolysis: electrocatalytic generation of oxygen gas at manganese oxide nanorods modified electrodes. Electrochem Commun 9:2082–2087
28. Morita M, Iwakura C, Tamura H (1979) The anodic characteristics of massive manganese oxide electrode. Electrochim Acta 24:357–362
29. Morita M, Iwakura C, Tamura H (1977) The anodic characteristics of manganese dioxide electrodes prepared by thermal decomposition of manganese nitrate. Electrochim Acta 22:325–328
30. Morita M, Iwakura C, Tamura H (1978) The anodic characteristics of modified Mn oxide electrode: Ti/RuO_x/MnO_x. Electrochim Acta 23:331–335
31. Robinson DM, Go YB, Greenblatt M, Dismukes GC (2010) Water oxidation by λ-MnO_2: catalysis by the cubical Mn_4O_4 subcluster obtained by delithiation of spinel $LiMn_2O_4$. J Am Chem Soc 132:11467–11469
32. Najafpour MM, Ehrenberg T, Wiechen M, Kurz P (2010) Calcium manganese(III) oxides ($CaMn_2O_4 \cdot xH_2O$) as biomimetic oxygen-evolving catalysts. Angew Chem Int Ed 49:2233–2237
33. Jiao F, Frei H (2010) Nanostructured manganese oxide clusters supported on mesoporous silica as efficient oxygen-evolving catalysts. Chem Commun 46:2920–2922
34. Yagi M, Narita K (2004) Catalytic O_2 Evolution from water induced by adsorption of $[(OH_2)(terpy)Mn(\mu\text{-}O)_2Mn(terpy)(OH_2)]^{3+}$ complex onto clay compounds. J Am Chem Soc 126:8084–8085
35. Narita K, Kuwabara T, Sone K, Shimizu K, Yagi M (2006) Characterization and activity analysis of catalytic water oxidation induced by hybridization of $[(OH_2)(terpy)Mn(\mu\text{-}O)_2Mn(terpy)(OH_2)]^{3+}$ and clay compounds. J Phys Chem B 110:23107–23114
36. Brimblecombe R, Swiegers GF, Dismukes GC, Spiccia L (2008) Sustained water oxidation photocatalysis by a bioinspired manganese cluster. Angew Chem Int Ed 47:7335–7338
37. Limburg J, Vrettos JS, Liable-Sands LM, Rheingold AL, Crabtree RH, Brudvig GW (1999) A functional model for O–O bond formation by the O_2-evolving complex in photosystem II. Science 283:1524–1527
38. Naruta Y, Sasayama M, Sasaki T (1994) Oxygen evolution by oxidation of water with manganese porphyrin dimers. Angew Chem Int Ed Engl 33:1839–1841
39. Gao Y, Åkermark T, Liu J, Sun L, Åkermark B (2009) Nucleophilic attack of hydroxide on a Mn^V Oxo complex: a model of the O–O bond formation in the oxygen evolving complex of photosystem II. J Am Chem Soc 131:8726–8727
40. Najafpour MM, Haghighi B, Ghobadi MZ, Sedigh DJ (2013) Nanolayered manganese oxide/poly(4-vinylpyridine) as a biomimetic and very efficient water oxidizing catalyst: toward an artificial enzyme in artificial photosynthesis. Chem Comm 49:8824–8826
41. Cheng F, Shen J, Peng B, Pan Y, Tao Z, Chen J (2011) Rapid room-temperature synthesis of nanocrystalline spinels as oxygen reduction and evolution electrocatalysts. Nat Chem 3:79–84
42. Singh RN, Singh JP, Cong HN, Chartier P (2006) Effect of partial substitution of Cr on electrocatalytic properties of $MnFe_2O_4$ towards O_2-evolution in alkaline medium. Int J Hydrogen Energy 31:1372–1378

43. Robinson DM, Go YB, Mui M, Gardner G, Zhang Z, Mastrogiovanni D, Garfunkel E, Li J, Greenblatt M, Dismukes GC (2013) Photochemical water oxidation by crystalline polymorphs of manganese oxides: structural requirements for catalysis. J Am Chem Soc 135:3494–3501
44. Takashima T, Hashimoto K, Nakamura R (2012) Mechanisms of pH-dependent activity for water oxidation to molecular oxygen by MnO_2 electrocatalysts. J Am Chem Soc 134:1519–1527
45. Takashima T, Hashimoto K, Nakamura R (2012) Inhibition of charge disproportionation of MnO_2 electrocatalysts for efficient water oxidation under neutral conditions. J Am Chem Soc 134:18153–18156
46. Takashima T, Yamaguchi A, Hashimoto K, Irie H, Nakamura R (2014) In situ UV-vis absorption spectra of intermediate species for oxygen-evolution reaction on the surface of MnO_2 in neutral and alkaline media. Electrochemistry 82:325–327
47. Umena Y, Kawakami K, Shen J-R, Kamiya N (2011) Crystal structure of oxygen-evolving photosystem II at a resolution of 1.9 Å. Nature 473:55–61
48. Yano J, Kern J, Sauer K, Latimer MJ, Puskar Y, Biesiadka J, Loll B, Saenger W, Messinger J, Zouni A, Yachandra VK (2006) Where water is oxidized to dioxygen: structure of the photosynthetic Mn_4Ca cluster. Science 314:821–825
49. Haumann M, Muller C, Liebisch P, Iuzzolino L, Dittmer J, Grabolle M, Neisius T, Meyer-Klaucke W, Dau H (2005) Structural and oxidation state changes of the photosystem II manganese complex in four transitions of the water oxidation Cycle ($S_0 \rightarrow S_1$, $S_1 \rightarrow S_2$, $S_2 \rightarrow S_3$, and $S_{3,4} \rightarrow S_0$) characterized by X-ray absorption spectroscopy at 20 K and room temperature. Biochemistry 44:1894–1908
50. Siegbahn PE (1827) Water oxidation mechanism in photosystem II, including oxidations, proton release pathways, O-O bond formation and O2 release. Biochim Biophys Acta 1003–1019:2013
51. Gatt P, Stranger R, Pace RJ (2011) Application of computational chemistry to understanding the structure and mechanism of the Mn catalytic site in photosystem II—a review. J Photochem Photobiol, B 104:80–93
52. Galstyan A, Robertazzi A, Knapp EW (2012) Oxygen-evolving Mn cluster in photosystem II: the protonation pattern and oxidation state in the high-resolution crystal structure. J Am Chem Soc 134:7442–7449
53. Kanda K, Yamanaka S, Saito T, Umena Y, Kawakami K, Shen J-R, Kamiya N, Okumura M, Nakamura H, Yamaguchi K (2011) Labile electronic and spin states of the $CaMn_4O_5$ cluster in the PSII system refined to the 1.9 Å X-ray resolution. UB3LYP computational results. Chem Phys Lett 506:98–103
54. Gatt P, Petrie S, Stranger R, Pace RJ (2012) Rationalizing the 1.9 Å crystal structure of photosystem II—a remarkable Jahn–Teller balancing act induced by a single proton transfer. Angew Chem Int Ed 51:12025–12028
55. Roelofs TA, Liang WC, Latimer MJ, Cinco RM, Rompel A, Andrews JC, Sauer K, Yachandra VK, Klein MP (1996) Oxidation states of the manganese cluster during the flash-induced S-state cycle of the photosynthetic oxygen-evolving complex. Proc Natl Acad Sci USA 93:3335–3340
56. Sproviero EM, Gascon JA, McEvoy JP, Brudvig GW, Batista VS (2008) A model of the oxygen-evolving center of photosystem II predicted by structural Refinement based on EXAFS Simulations. J Am Chem Soc 130:6728–6730
57. Mazin II, Khomskii DI, Lengsdorf R, Alonso JA, Marshall WG, Ibbreson RM, Podlesnyak A, Martínez-Lope MJ, Abd-Elmeguid MM (2007) Charge ordering as alternative to Jahn-Teller distortion. Phys Rev Lett 98:176406
58. Mizokawa T, Khomskii DI, Sawatzky GA (2000) Spin and charge ordering in self-doped Mott insulators. Phys Rev B 61:11263–11266
59. Amin M, Vogt L, Vassiliev S, Rivalta I, Sultan MM, Bruce D, Brudvig GW, Batista VS, Gunner MR (2013) Electrostatic effects on proton-coupled electron transfer in oxomanganese complexes inspired by the oxygen-evolving complex of photosystem II. J Phys Chem B 117:6217–6226

60. Meyer TJ, Huynh MH, Thorp HH (2007) The possible role of proton-coupled electron transfer (PCET) in water oxidation by photosystem II. Angew Chem Int Ed 46:5284–5304
61. Ogata K, Yuki T, Hatakeyama M, Uchida W, Nakamura S (2013) All-atom molecular dynamics simulation of photosystem II embedded in thylakoid membrane. J Am Chem Soc 135:15670–15673
62. Yamaguchi A, Inuzuka R, Takashima T, Hayashi T, Hashimoto K, Nakamura R (2014) Regulating proton-coupled electron transfer for efficient water splitting by manganese oxides at neutral pH. Nat Commun doi:10.1038/ncomms5256
63. Medina-Ramos J, Oyesanya O, Alvarez JC (2013) Buffer effects in the kinetics of concerted proton-coupled electron transfer: the electrochemical oxidation of glutathione mediated by $[IrCl_6]^{2-}$ at variable buffer pK_a and concentration. J Phys Chem C 117:902–912
64. Jencks WP (1972) Requirements for general acid-base catalysis of complex reactions. J Am Chem Soc 94:4731–4732
65. Jencks WP (1972) General acid-base catalysis of complex reactions in water. Chem Rev 72:705–718
66. Russell MJ, Hall AJ (2002) Chemiosmotic coupling and transition element clusters in the onset of life and photosynthesis. The Geochemical News 113:6–12
67. Sauer K, Yachandra VK (2002) A possible evolutionary origin for the Mn_4 cluster of the photosynthetic water oxidation complex from natural MnO_2 precipitates in the early ocean. Proc Natl Acad Sci USA 99:8631–8636
68. Armstrong FA (2008) Why did nature choose manganese to make oxygen? Phil Trans R Soc B 363:1263–1270
69. http://pubs.usgs.gov/fs/2002/fs087-02/
70. Dismukes GC, Klimov VV, Baranov SV, Kozlov YN, Dasgupta J, Tyryshkin A (2001) The origin of atmospheric oxygen on earth: the innovation of oxygenic photosynthesis. Proc Natl Acad Sci USA 98:2170–2175
71. Lane N (2010) The rollercoaster ride to an oxygen-rich world. New Scientist 205:2746
72. Kirschvink JL, Gaidos EJ, Bertani LE, Beukes NJ, Gutzmer J, Maepa LN, Steinberger RE (2000) Paleoproterozoic snowball earth: extreme climatic and geochemical global change and its biological consequences. Proc Natl Acad Sci USA 97:1400–1405
73. Fan X, Hou J, Sun D, Xi S, Liu Z, Du J, Luo J, Tao C (2013) Mn-oxides catalyzed periodic current oscillation on the anode. Electrochim Acta 102:466–471
74. Olexová A, Melicherčík M, Treindl L (1997) Oscillatory oxidation of Mn(II) ions by hexacyanoferrates(III) and bistability in the reduction of MnO_2 by hexacyanoferrates(II) in a CSTR. Chem Phys Lett 268:505–509
75. Tributsch H (1994) The challenge of non-linear and co-operative mechanisms for electrocatalysis. Electrochim Acta 39:1495–1502